Journal of Engineering Research and Education
Volume 10, 2018 [91-100]

The Effects of Different Load Power Factors on the Performance of Distance Relay

Muhd Hafizi Idris*, Mohd Rafi Adzman and Mohammad Faridun Naim Tajuddin

Centre of Excellence for Renewable Energy (CERE), School of Electrical System Engineering Universiti Malaysia Perlis, 02600, Arau, Malaysia.

ABSTRACT

A Distance Relay typically used as main protection relay to protect transmission line from any type of fault. It is very sensitive to voltage and current variation because it uses the impedance measurement principle to detect fault occurrence and fault zone. The impedance measured by distance relay might be different from the actual fault impedance from relay point until fault point because of various factors and one of it is load variation. This research aims to analyze the effects of load power factor variation on the accuracy of distance relay. Transmission line, three-phase source, three-phase load and distance relay were modeled using Matlab/Simulink software. Single line-to-ground (SLG) fault algorithm and Mho characteristic have been chosen in this research to analyze the effects of load variation. Power factor of the load was varied by varying load reactive power to be inductive and capacitive. From the results, it can be concluded that distance relay will be mal-operated for faults near zone reach setting when power factor is less than unity for either lagging or leading conditions.

Keywords: Distance Relay, Impedance Measurement, Load Power Factor, Mal-Operation, Power System.

1. INTRODUCTION

Transmission line is one of important components in power system. It can be in the form of overhead line or underground cable. Transmission line must be protected from any type of fault to maintain the reliability and security of power system. There are two types of relay used to protect transmission line, which are main and backup protection relays. Typical relays used as main protection relay are distance and current differential relays. Distance relay measures the apparent impedance from relay point until fault point and send the trip signal when the computed impedance is less than the set impedance (WG B5.15, 2008). For current differential relay, it measures the differential current between local and remote phase currents. When a fault occurred at transmission line, differential current will be higher than the set pickup current and relay will send trip signal to isolate the line (Werstiuk, 2010).

Figure 1 shows the basic distance protection scheme. The inputs for distance protection relay are three phase current and voltage phasors (Idris, Hardi, & Hasan, 2013). Three phase current phasors are taken from current transformer (CT) while three phase voltage phasors are taken from voltage transformer (VT). Distance relay uses impedance calculation algorithms to detect the faults within the protected zone. Each type of fault has its own algorithm to calculate the impedance.

* Corresponding Author: *hafiziidris@unimap.edu.my*

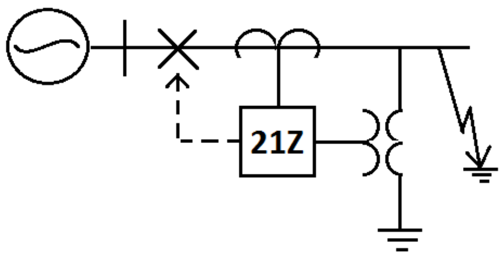

Figure 1. Basic distance protection scheme (Idris *et al.*, 2013).

Table 1 shows the algorithms used to calculate the impedance for each type of fault (Sidhu, Ghotra, & Sachdev, 2000). When a fault occurred at transmission line, distance relay will first determine the type of fault using internal phase selection feature. Then, it will use the correct algorithm to calculate the fault impedance (Utsumi et al., 2011).

Table 1 Fault impedance calculation algorithms for different fault types

Fault Types	Fault Impedance Calculation Algorithms
AG	$V_A/(I_A+3k_0I_0)$
BG	$V_B/(I_B+3k_0I_0)$
CG	$V_C/(I_C+3k_0I_0)$
AB OR ABG	$(V_A-V_B)/(I_A-I_B)$
BC OR BCG	$(V_B-V_C)/(I_B-I_C)$
CA OR CAG	$(V_C-V_A)/(I_C-I_A)$

Where;
A, B and C indicate faulty phases.
G indicates ground fault.
VA, VB and VC indicate voltage phasors
IA, IB and IC indicate current phasors
Z0 = line zero-sequence impedance
Z1 = line positive-sequence impedance
k0 = residual compensation factor where k0 = (Z0-Z1)/Z1.
I0 = zero-sequence current.

There are many types of distance relay characteristics such as Plain, Mho, Offset Mho, Polarized Mho, Reactance, Quadrilateral and many other characteristics. Each type of characteristic is dedicated for different application and transmission line configuration (Alstom, 2011). Figure 2 shows the Mho characteristic which is typically used to protect long transmission line where fault resistance, Rf do not has much effect on the accuracy of distance relay (Mason, 1956).

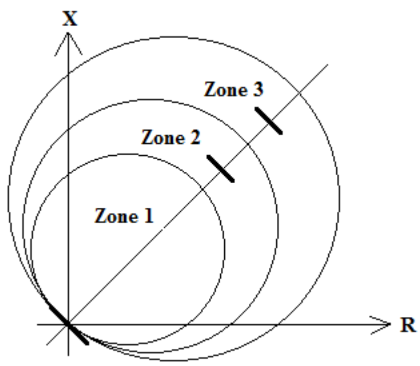

Figure 2. Mho characteristic.

Distance relay segregates the connected transmission lines into different zones of protection typically zone 1, zone 2, zone 3, zone 3 offset or zone 3 reverse, load area and power swing area. These zones are coordinated in sequence starting from zone 1 depending on the calculated distance or impedance to the fault point. The nearer the fault to relay terminal, the higher the fault current and the smaller the fault impedance will be thus faster tripping signal is required to isolate the fault. For zones more than zone 1, delayed tripping signals are set to act as backup for zone 1 and also when other dedicated protection relays/zones fail to isolate the fault (Mason, 1956).

Distance relay measures the apparent fault impedance, therefore it is very sensitive to the variation of voltage and current phasors. The computed fault impedance by distance relay might be different from the actual impedance until fault point. Among the factors that can affect the accuracy of impedance measurement by distance relay are transmission line mutual impedance, current transformer saturation, high fault resistance, source impedance ratio, transmission line charging current, remote current contribution, and FACTs devices operation (Calero, 2015; Elmitwally, 2010; Elmore, 2003; Erezzaghi & Crossley, 2003; Mooney, 2008; Xue, Finney, & Le, 2013). Fault impedance will produce error in impedance measurement of traditional ground distance relay and caused the distance relay to be under-reached if fault resistance is not accordingly considered, thus fault will be tripped at a delayed time instead of instantaneously (Alstom, 2011).

2. METHODOLOGY

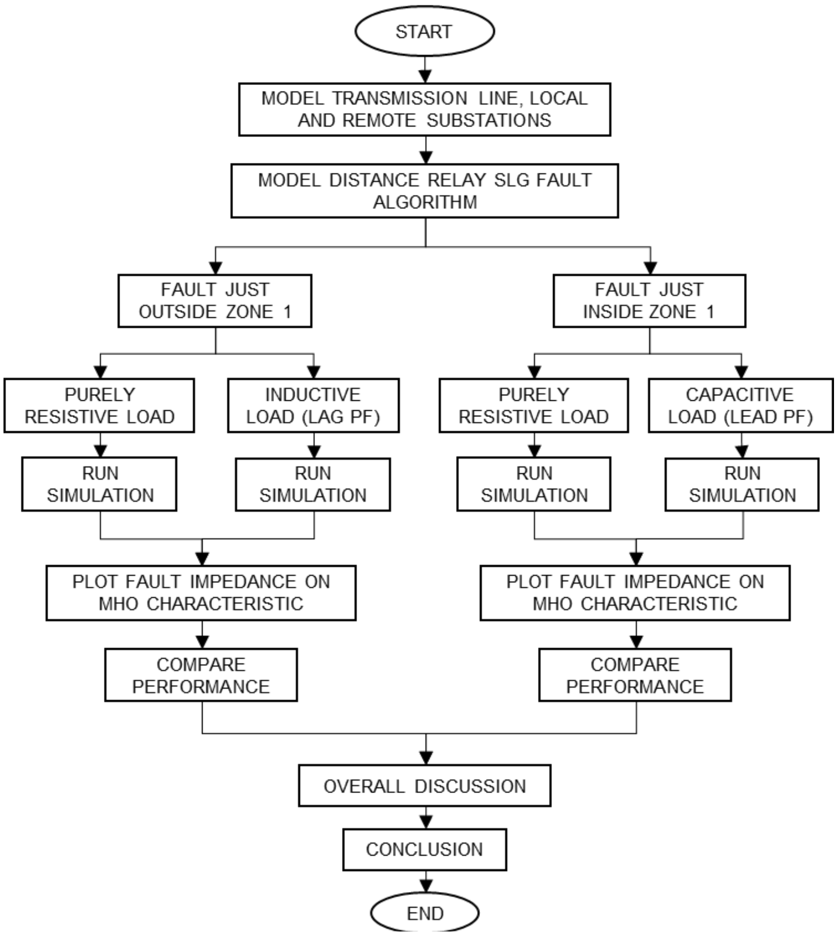

Figure 3. Flow chart of research.

The flow chart of the research is shown by Figure 3. The project started with modelling power system network using Matlab/Simulink sofware. Figure 4 shows the single line diagram of the power system network, connected distance relay (21Z) locations, and the selected setting of zone 1 for both local and remote substations which is 80%.

Transmission line, three-phase source, three-phase load, power factor calculation, and distance relay are the main components of the power system network. Figure 5 shows the developed model of power system network using Simulink. The current and voltage signals which are the inputs for distance relay are taken from three-phase measurement which represents the current transformer (CT) and voltage transformer (VT) in the actual substation.

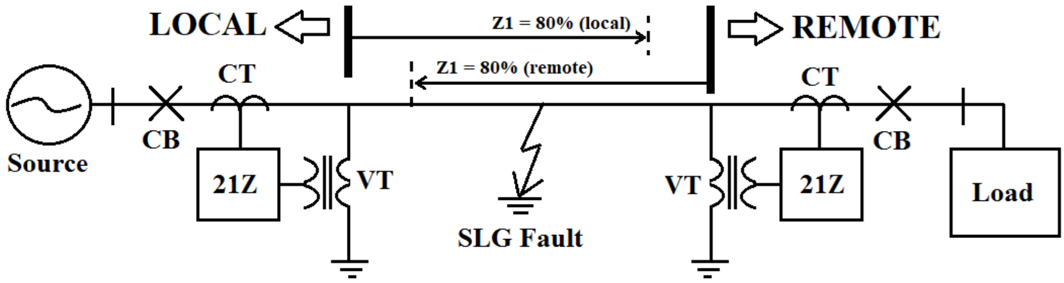

Figure 4. Single line diagram with distance relay locations and zone 1 reach setting for both locations.

Table 2 shows the parameters used for the power system network. The transmission line selected is a spur transmission line where one end of the line is connected to an equivalent three-phase source and the other end is connected to a three-phase load. The reactive component of the load was varied to change the load power factor.

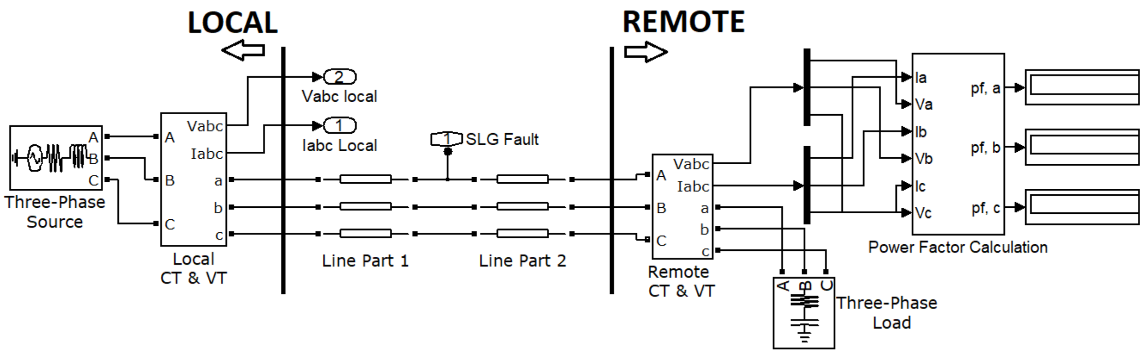

Figure 5. Network subsystem model.

Table 2 Power system network parameters

Parameters	Value
Rated voltage, Vrms	132 kV
Nominal frequency, f	50 Hz
Local substation short circuit power, $S_{s/c}$	1.044 GVA
Local substation X/R ratio	1
Line positive sequence resistance, R1	0.045531917 Ω/km
Line zero sequence resistance, R0	0.151489359 Ω/km
Line positive sequence inductance, L1	0.0006176566224 H/km
Line zero sequence inductance, L0	0.001533982723 H/km
Line length, L	47 km

After there was no error from the simulation of the developed power system network model, next step was developing the distance relay fault impedance algorithm for single line-to-ground (SLG) fault. To detect the fault zone, Mho characteristic has been chosen as the relay's characteristic. In order for the model to compute the fault impedance during fault occurrence, it requires the voltage and current phasors (magnitudes and angles of the signals) during fault condition. First, the harmonics in voltage and current signals will be filtered to remove high frequency components which might appear during fault occurrence due to fault arc using Analogue Low Pass Filter (cutoff frequency, fcutoff = 628 rad/s) subsystem. Then, the filtered signals will be sent to Fourier Analysis subsystem to compute the magnitudes and angles of the voltage and current signals.

The magnitudes and angles (in radian) of voltage and current signals then will be transferred to Apparent Impedance Algorithm subsystem to compute the fault impedance seen by distance relay. Apparent impedance algorithm used is for single line-to-ground fault as shown in Table 1. Computed fault resistance and fault reactance will be transferred to the workspace and plotted onto impedance diagram to determine the location of fault (inside or outside of zone 1). Figure 6 shows the overall model of the project while Figure 7 shows the blocks inside apparent impedance algorithm subsystem.

To analyze the effects of load power factor variation on distance relay operation, fault has been simulated at two locations which were one fault at just outside zone 1 and the other one fault at just inside zone 1. This research only focus on zone 1 but the same method can be carried out for other zones. For each fault location, load was varied for two conditions which were one purely resistive load and the other one was inductive load (for fault just outside zone 1) or capacitive load (for fault just inside zone 1).

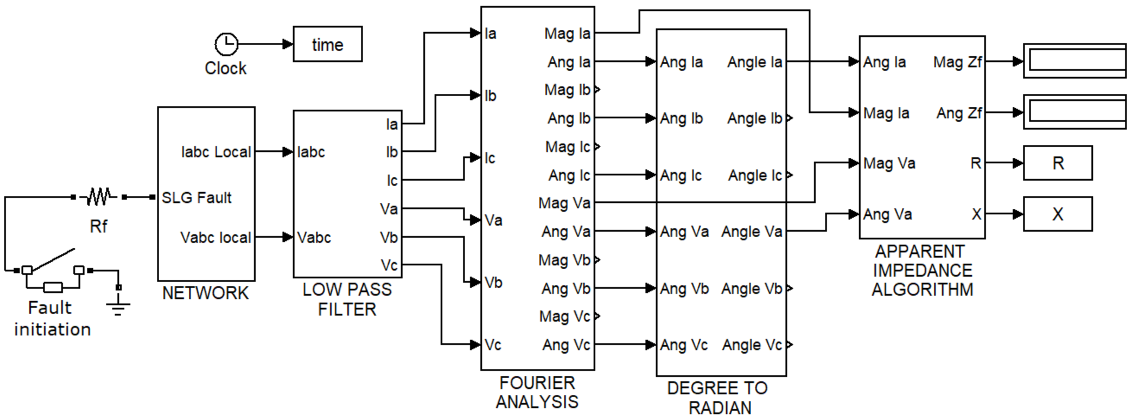

Figure 6. Overall model of the project.

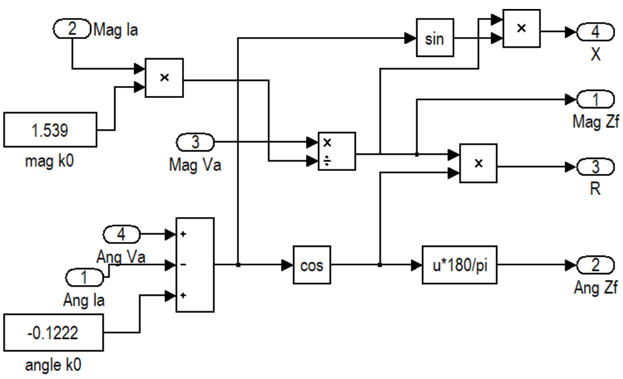

Figure 7. Apparent impedance algorithm subsystem.

Then, the simulations were run for both conditions (purely resistive and inductive or capacitive load) for each fault location and fault impedance locus was plotted onto Mho characteristics for both conditions. From the fault impedance locus, analysis was carried out whether the change of load conditions from purely resistive load to inductive or capacitive load will make distance relay to be under-reached or over-reached (where relay will be mal-operated).

3. RESULTS AND DISCUSSION

To see the effects of power factor variation on distance relay performance for fault near zone 1 reach boundary, fault was simulated at two different locations which are at 38.5 km (measured fault impedance just outside the zone 1 reach boundary) and at 38 km (measured fault impedance just inside the zone 1 reach boundary). The fault locations were referred from local substation. For each fault location, power factor was varied for three conditions which are power factor equal to 1, 0.9 and 0.8.

Table 3 shows the results of the measured fault impedance for different load power factors for fault at 38.5 km from local substation. The load was changed from purely consuming active power (case 1) to consuming both active and inductive reactive powers (case 2 and 3). The effect of changing the load type was by changing the power factor from unity power factor to 0.9 and 0.8 lagging power factors. It can be seen that, the lower the power factor for lagging conditions, the lower the value of measured fault resistance (R), fault reactance (X), and fault impedance (Z).

Table 3 R-G fault at 38.5 km

Case	pf	P (MW)	Q_L (MVar)	Q_C (MVar)	Lagging / Leading	R (Ω)	X (Ω)	Z (Ω)
1	1	30	0	0	-	3.021	6.733	7.38
2	0.9	30	14.53	0	lagging	2.927	6.686	7.299
3	0.8	30	22.5	0	lagging	2.875	6.656	7.25

Where;

pf = power factor
P = Active power
Q_L = Inductive reactive power
Q_C = Capacitive reactive power

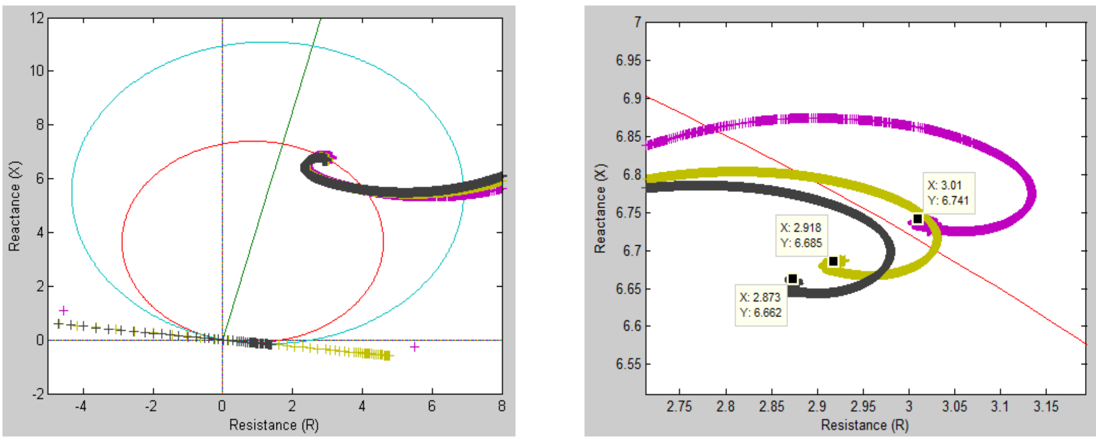

(a) (b)

Figure 8. Measured fault impedance locus for all three cases when fault occurred at 38.5 km from local substation.

Figure 8(a) shows the measured fault impedance locus inside impedance diagram while Figure 8(b) shows the scaled up version of measured fault impedance locus for all three cases for fault at 38.5 km. From the locus in Figure 8(b), it can be concluded that, when power factor decreasing in lagging conditions, then the measured impedance is low, thus the impedance will be over-reached when the actual fault impedance is just outside the reach boundary. This condition will change the relay decision from sending the tripping signal at a delayed time (zone 2) to sending the tripping signal at instantaneous time (zone 1) which is not desired.

Table 4 shows the results of the measured fault impedance for different load power factors for fault at 38 km. The load was changed from purely consuming active power (case 1) to consuming both active and capacitive reactive powers (case 2 and 3). The effect of changing the load type was by changing the power factor from unity power factor to 0.9 and 0.8 leading power factors. It can be seen that, the lower the power factor for leading conditions, the higher the value of measured fault resistance (R), fault reactance (X), and fault impedance (Z).

Table 4 R-G fault at 38 km

Case	pf	P (MW)	Q_L (Mvar)	Q_C (MVar)	Lagging / Leading	R (Ω)	X (Ω)	Z (Ω)
1	1	30	0	0	-	2.986	6.642	7.282
2	0.9	30	0	14.53	leading	3.094	6.694	7.374
3	0.8	30	0	22.5	leading	3.156	6.719	7.423

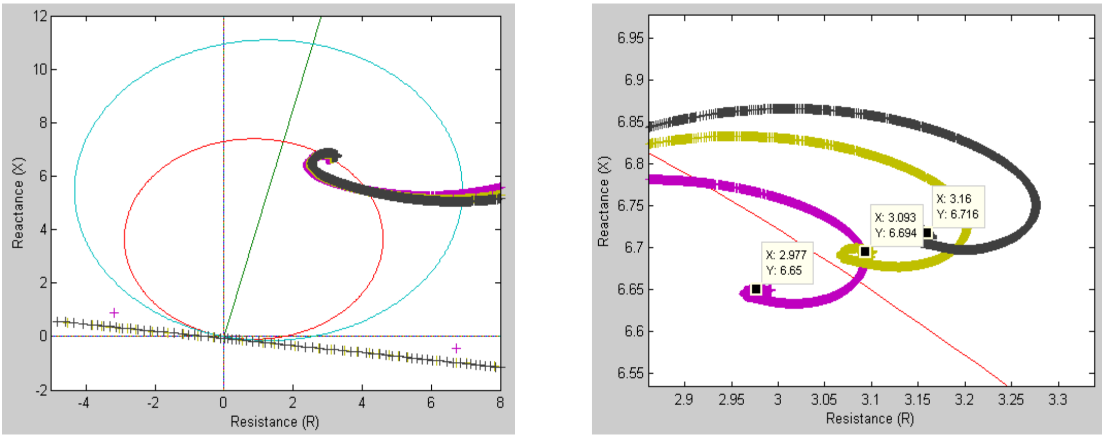

(a) **(b)**

Figure 9. Measured fault impedance locus for all three cases when fault occurred at 38 km from local substation.

Figure 9(a) shows the measured fault impedance locus inside impedance diagram while Figure 9(b) shows the scaled up version of measured fault impedance locus for all three cases for fault at 38 km. From the locus in Figure 9(b), it can be concluded that, when power factor becoming lower in leading conditions, the impedance measured will be higher, thus the impedance will be under-reached when the actual fault impedance is just inside the reach boundary. This condition will change the relay decision from sending the tripping signal at instantaneous time (zone 1) to sending the tripping signal at a delayed time (zone 2) which is not desired.

4. CONCLUSION

This section conclude the results discussed in the previous section. From all tables and figures in results and discussion, it can be concluded that for lower power factor in lagging condition, it will make the distance relay to be over-reached when actual fault impedance is just outside the reach boundary of zone 1. Whereas, for lower power factor in leading condition, it will make the distance relay to be under-reached when actual fault impedance is just inside the reach boundary of zone 1.

Both situations affect the performance of distance relay in making decision to send the tripping signal because the actual fault impedance at the line will be seen differently by the relay as shown by the measured fault impedance in the previous section. Thus, it can be said that the distance relay will be mal-operated for faults near zone 1 reach setting when power factor less than unity for either lagging or leading conditions.

The proposed solutions to prevent distance relay from mal-operated (under-reached or over-reached) due to low power factor can be divided into external and internal solutions. For external solution, utility company and high load connected customer have to install appropriate compensation components such as installing capacitor or reactor banks to improve power factor near unity when their system or load has been proved as the reason for low power factor. For internal solution, numerical distance protection relay can add internal power factor calculation algorithm. When power factor is less than unity, internal compensation can be made such as adding mutual capacitance or reactance. Apparent fault impedance only will be computed after internal compensation has been made.

REFERENCES

[1] Alstom, Network Protection & Automation Guide (May). Alstom Grid, (2011).

[2] Calero, F. Mutual Impedance in Parallel Lines - Protective Relaying and Fault Location Considerations. In 34th Annual Western Protective Relay Conference. (2015). Retrieved from *https://cdn.selinc.com/assets/Literature/Publications/Technical Papers/6283_MutualImpedance_FC_20150513_Web.pdf?v=20151124-113324*

[3] Elmitwally, A. Effect of FACT Devices on Distance Relay. The Online Journal on Power and Energy Engineering (OJPEE) **2**, 2 (2010). 196–203.

[4] Elmore, W. A. Protective Relaying: Theory and Applications (2nd ed.). CRC Press, (2003).

[5] Erezzaghi, M. E., & Crossley, P. A., The Effect of High Resistance Faults on a Distance Relay. In IEEE Power Engineering Society General Meeting (IEEE Cat. No.03CH37491) (pp. 2128–2133). Toronto, Ont., Canada: IEEE, (2003).

[6] Idris, M. H., Hardi, S., & Hasan, M. Z., Teaching Distance Relay using Matlab/Simulink Graphical user Interface. Procedia Engineering **53** (2013) 264–270.

[7] Mason, C. R., The Art & Science of Protective Relaying. Wiley, (1956).

[8] Mooney, J., Distance Element Performance Under Conditions of CT Saturation. In 2008 61st Annual Conference for Protective Relay Engineers, College Station, TX, USA: IEEE. (2008) 491–497.

[9] Sidhu, T. S., Ghotra, D. S., & Sachdev, M. S., A Fast Distance Relay using Adaptive Data Window Filters. In Power Engineering Society Summer Meeting. Seattle, WA, USA, (2000).

[10] Utsumi, T., Nakatsuka, T., Takani, H., Amoh, H., Kawano, F., & Beaumont, P., Faulted phase selection function based upon impedance comparison in a distance protection relay. In 2011 International Conference on Advanced Power System Automation and Protection, Beijing, China: IEEE, (2011) 314–319.

[11] Werstiuk, C., The Relay Testing Handbook: End-to-End Testing (7th ed.). Valence Electrical Training Services LLC, (2010).

[12] WG B5.15., Modern Distance Protection Functions and Applications. ELECTRA, (2008) 39–47.

[13] Xue, Y., Finney, D., & Le, B., Charging Current in Long Lines and High-Voltage Cables – Protection Application Considerations. In 67th Annual Georgia Tech Protective Relaying Conference. Atlanta, Georgia: American Electric Power and Schweitzer Engineering Laboratories, Inc. (2013). Retrieved from *https://cdn.selinc.com/assets/Literature/Publications/Technical Papers/6574_ChargingCurrent_DF_20120914_Web2.pdf?v=20151124-160900*